Domain wall depinning from notches using combined in- and out-of-plane magnetic fields

Jelle J. W. Goertz, , Grazvydas Ziemys, , Irina Eichwald, , Markus Becherer, , Henk J. M. Swagten, and , and Stephan Breitkreutz-v. Gamm

Citation: AIP Advances **6**, 056407 (2016); doi: 10.1063/1.4944698
View online: http://dx.doi.org/10.1063/1.4944698
View Table of Contents: http://aip.scitation.org/toc/adv/6/5
Published by the American Institute of Physics

Domain wall depinning from notches using combined in- and out-of-plane magnetic fields

Jelle J. W. Goertz,[1,a] Grazvydas Ziemys,[2] Irina Eichwald,[2]
Markus Becherer,[2] Henk J. M. Swagten,[1] and Stephan Breitkreutz-v. Gamm[2]
[1]*Department of Applied Physics, Eindhoven University of Technology, P.O. Box 513, 5600 MB, Eindhoven, The Netherlands*
[2]*Institute for Technical Electronics, Technical University of Munich, Munich, Germany*

(Presented 12 January 2016; received 5 November 2015; accepted 2 February 2016; published online 18 March 2016)

Controlled domain wall motion and pinning in nanowires with perpendicular magnetic anisotropy are of great importance in modern magnetic memory and logic devices. Here, we investigate by experiment the DW pinning and depinning from a notch in a magnetic nanowire, under the influence of combined in- and out-of-plane magnetic fields. In our experiment, the perpendicular magnetization of the Co/Pt nanowires is tilted with the help of sub-μs in-plane field pulses generated by an on-chip coil. Consequently, the energy density of the DW is decreased and the depinning field of the notch is reduced. A theoretical model is applied and compared to the measurement results. The DW depinning mechanism and the DW type are further investigated by micromagnetic simulations. [http://dx.doi.org/10.1063/1.4944698]

I. INTRODUCTION

Domain wall (DW) motion and pinning in nanowires with perpendicular magnetic anisotropy (PMA) are of great interest in next generation magnetic memory and logic devices.[1–3] Moreover, the use of DW motion and pinning in magnetic nanowires may accelerate a high storage and computing density and additionally low energy consumption in perpendicular Nanomagnetic Logic (pNML) systems. Here, notches can be used to control the signal flow in the interconnecting nanowires.[4] The inherent nonvolatility of the magnets in pNML and the pipelined signal processing between logic gates according to a clocking field makes pNML suitable to a wide range of architectures and signal processing.[5,6]

Generally, in digital logic circuits signals are transmitted, synchronized and buffered to facilitate complex logic circuitry. In pNML, usually nanowires with perpendicular magnetic anisotropy (PMA) are used as interconnects to transfer and control signals. Storing signals within the nanowire is required to buffer magnetic domains as input states in logic gates.

Therefore geometrical deformations (e.g. notches) are patterned within the nanowire and the magnetic domain is pinned at such a notch. To depin a magnetic domain from the notch, an additional out-of-plane field, e.g. by surrounding magnets, has to be applied.[4,7] In this way the signal flow is controlled by additional fields that cause the depinning of the DW.

Lowering this depinning field by the use of already applied fields within the logic system can be of great importance in future pNML systems. We will show by experiment that we can reduce the depinning field significantly by adding an in-plane field pulse to the notch to control the DW motion through it. The findings are substantiated by theoretical calculations and micromagnetic simulations.

[a]j.j.w.goertz@student.tue.nl; Exchange Student at the Institute for Technical Electronics, Technical University of Munich, Munich, Germany

II. THEORY

A. Domain wall pinning at notches

Geometrical deformations (e.g., notches or edge roughness) are able to induce the necessary energy barrier with a pinning potential in PMA nanowires in order to control the signal flow in pNML systems.[5,4,8]

When a DW in the nanowire is moving towards such a notch, the DW minimizes its energy by settling down in the notch in case of no external fields.[8,9] The energy to overcome the barrier of the notch can be supplied by the Zeeman energy of external fields[10,11] and is given by

$$E_{zeeman} = -\mu_0 \int \vec{M} \cdot \vec{H}_{ext} dV = -\mu_0 M_s H_z \cdot A \cdot t, \tag{1}$$

with M_s the saturation magnetization, $H_z = B_z/\mu_0$ the external applied magnetic field in z-direction, A the domain area and t the magnetic layer thickness. The energy of the domain wall itself, however, is given by

$$E_{DW} = \sigma_w \cdot t \cdot l_w, \tag{2}$$

with DW length l_w and a DW energy density[10] for a 180° Bloch wall in thin films equal to $\sigma_w = \pi\sqrt{2}\sqrt{A_{ex}K_{eff}}$ with exchange stiffness A_{ex} and effective anisotropy K_{eff}. Due to these energy contributions the pinned DW is bent to an arc of circle to maximize its area A and minimize its length l_w. Once the out-of-plane magnetic field B_z reaches the so-called depinning field B_{dep}, the DW will be depinned and released from the notch. The competition between the Zeeman energy E_{zeeman} and the DW energy E_{DW} without any further energy contribution (e.g. thermal energy) yields the field for depinning from a triangular notch given by[8]

$$B_{dep} = B_{int} + \frac{\sigma_w \sin(\alpha)}{2M_s(h + \frac{1}{2}\delta_w \sin(\alpha))} \tag{3}$$

with the intrinsic field B_{int} for DW propagation at 0 Kelvin, the notchs apex angle α, the notch width h and DW width $\delta_w = \pi\sqrt{2}\sqrt{A_{ex}/K_{eff}}$ as indicated in Fig. 1. The trapezoidal shape of the investigated double-sided notch of Fig. 1(a) is modeled by 2 triangular shaped, single-sided notches.[7]

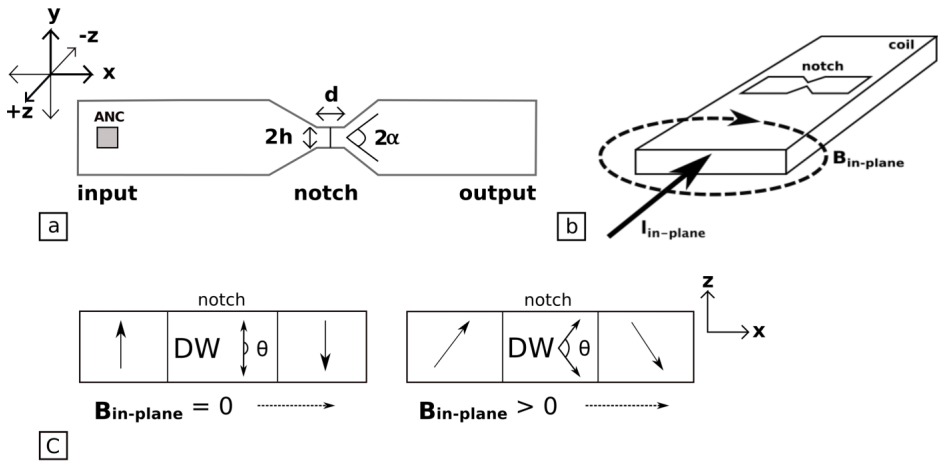

FIG. 1. Sketch of the experimental setup. a) Magnetic nanowire with ANC on the left (input) side to nucleate a DW and a notch of width $2h$ and apex angle 2α to pin the DW due to its energy barrier. b) Fabricated structure using a nanowire with notch on top of the current wire, which produces well-defined in-plane field-pulses at the position of the notch. c) Side view of the nanowire showing the magnetic moments before and after the notch with and without an applied in-plane field to reduce the DW angle θ.

B. Decreasing domain wall angle using in-plane fields

The DW energy density is not only dependent on the DW type (e.g., Bloch or Néel) but also on its DW angle (see Fig. 1(c)) via the following relation[10]:

$$\sigma_{w,\theta}(\theta) = \sigma_{w,180^\circ} \sin^2\left(\frac{\theta}{2}\right), \tag{4}$$

with $\sigma_{w,180^\circ}$ the DW energy for a 180° DW and θ the DW angle as defined in Fig. 1(c). Applying an in-plane magnetic field $B_{in-plane}$ tilts the magnetization of the structure according to the applied field and therefore lowers θ and the corresponding DW energy density. Since the depinning field from the notch is linearly dependent on $\sigma_{w,\theta}(\theta)$, we can lower this out-of-plane depinning field by applying an additional in-plane field to decrease θ.

The total applied field together with the effective anisotropy determines the actual DW angle in the notch. The Stoner-Wohlfahrt[11] theorem and first order Taylor expansion can is used to calculate the DW angle[12,13]:

$$\cos(\tilde{\theta}) = 1 - \frac{(M_s B_{eff})^2}{2(2K_{eff} + M_s B_{eff})^2}\phi^2. \tag{5}$$

with the effective field $B_{eff} = \sqrt{B_{in-plane}^2 + B_z^2}$ the combination of the in- and out-of-plane field, ϕ the angle between B_{eff} and the film normal (z-axis) and $\tilde{\theta}$ the angle between the final magnetization and film normal. Consequently, $\theta/2 = \pi/2 - \tilde{\theta}$ and thus $\cos(\tilde{\theta}) = \sin(\theta/2)$.

III. SIMULATION

To investigate the DW depinning behaviour, non-thermal (0 Kelvin) micromagnetic simulations are carried out with OOMMF[14] simulation software using the following nanowire parameters: $M_s = 7.23 \cdot 10^5$ A/m, $A_{ex} = 1.3 \cdot 10^{-11}$ J/m, $2\alpha = 90^\circ$, $2h = 50$ nm, and no DMI $D = 0$. Fig. 2 shows the simulated depinning field B_{dep} as function of the in-plane field $B_{in-plane}$ for different anisotropies K_u of the nanowire. Clearly an in-plane field $B_{in-plane}$ causes a decrease in the depinning field B_{dep} as expected, since the DW angle and its energy density is decreased.

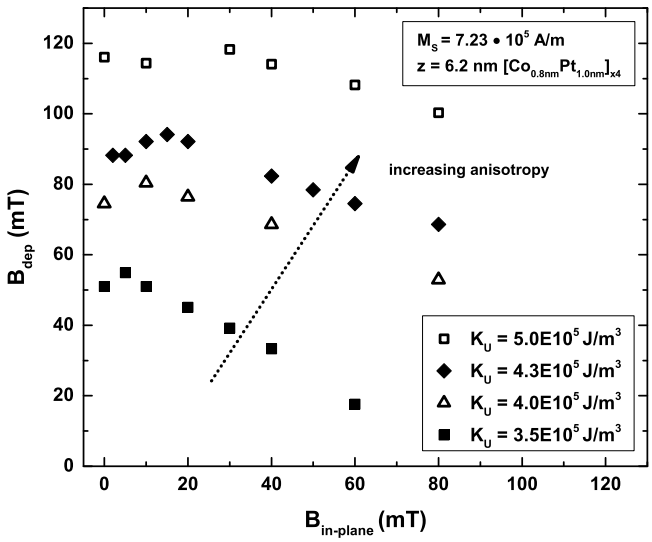

FIG. 2. Simulation results of the depinning field B_{dep} as function of an applied in-plane field $B_{in-plane}$. The out-of-plane depinning field is lowered when applying an in-plane field. For larger anisotropies larger depinning fields are needed to switch and depin the domain. A small increase in B_{dep} is observed for low $B_{in-plane}$ due to a change in DW type.

Furthermore the depinning field is higher for larger anisotropies, and the effect of the in-plane field is reduced as more energy is required to tilt the magnetic moments (compare eq. (5)).

Interestingly, for relatively small in-plane fields ($B_{in-plane} < 10 \ldots 15\,\mathrm{mT}$), B_{dep} is slightly increasing with $B_{in-plane}$ due to a change in DW type. The appearance of a Bloch wall as well as a Néel wall is geometry dependant. In our thin film notch geometry a combination of these two types is energetically most favorable. This can also be seen in Figure 3, where the simulated (local) magnetization state at the notch for different in-plane fields $B_{in-plane}$ is shown.

The DW type clearly depends on the applied in-plane field and is pushed from Bloch wall into a Néel wall for higher $B_{in-plane}$. Due to this transition, the DW energy and thus energy barrier is increased due to the larger Néel wall energy density. The larger DW energy density increases the depinning field according to eq. (3).

If the in-plane field is even further increased (e.g. $B_{in-plane} > 15\,\mathrm{mT}$ at $K_u = 4.0 \cdot 10^5 \mathrm{J/m^3}$) the effect of tilting the magnetic moments is increased. Hence, the DW energy density is also decreased due to a lower DW angle. This latter effect will become stronger for higher in-plane fields and will be dominant in this regime.

IV. EXPERIMENTS

A. Fabrication

For our experiment, we used an RF magnetron sputtered $Ti_{1nm}Pt_{3nm}[Co_{0.8nm}Pt_{1nm}]_{x4}Pt_{3nm}$ magnetic multilayer film deposited on a $Ti_{3nm}Cu_{500nm}Ti_{3nm}Al_{150nm}$ coil with a dielectric planarization layer on top of it. The coil is used to generate the in-plane field pulses. The nanowire with notch is fabricated by focused ion beam (FIB) lithography using a PMMA photoresist and ion beam etching with an evaporated Ti hard mask. The artificial nucleation center (ANC) of $40 \cdot 40\,\mathrm{nm}^2$ is fabricated by partial FIB irradiation and is used to control the DW injection on the input side.[15,16] In the notch, the 600 nm wide nanowire is reduced to $2h = 54\,\mathrm{nm}$, the apex angle $2\alpha \approx 51.5°$.

Figure 4 shows a scanning electron microscopy (SEM) image of the fabricated nanowire with notch. The ANC at the left side provides controlled DW nucleation and injection with field strength B_{nuc} at lower fields than the depinning field from the notch, $B_{nuc} < B_{dep}$.

B. Method

Wide-field magneto-optical-kerr-effect (MOKE) microscopy is used to image the domains in the nanowire and determine the depinning field. The out-of-plane field is generated with an external

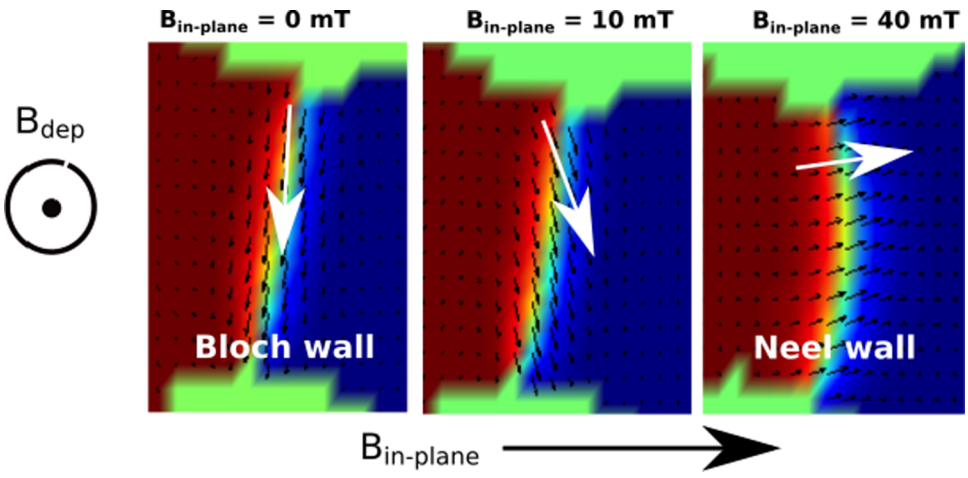

FIG. 3. Domain wall type at the notch for different strengths of the applied in-plane field. The blue and red colors give the out-of-plane magnetization. The black arrows show the local magnetization, and DW type, at the notch. The large white arrow is a guide to the eye for the magnetization at the notch. At zero in-plane field a Bloch wall appears with lowest energy. For higher in-plane fields the Néel wall appears more energetically favourable.

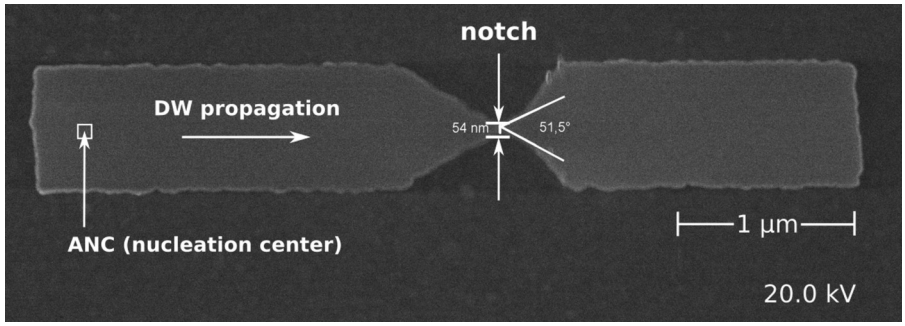

FIG. 4. SEM image of the fabricated nanowire with notch investigated in the experiment. The ANC at the left is used to nucleate a DW and inject it into the nanowire.

electromagnet, whereas the in-plane field pulses are generated with the on-chip current wire as drawn in Figure 1(b). The in-plane field pulses are generated by current pulses with a current density in the range of $j = 1 \ldots 3 \cdot 10^{11}\,\mathrm{A \cdot m^{-2}}$ and a pulse duration in the range of 200 ns, which doesn't lead to any significant problems of localized heating and eventually burning the wiring. The in-plane magnetic field components generated by the current wire are determined with the Finite Element Method Magnetics (FEMM) software,[17] which deduces a linear relation between the pulsed current $I_{in-plane}$ and $B_{in-plane}$ (additional out-of-plane components ΔB_z are also taken into account).

In the experiment, first the DW is nucleated at the ANC by a pure out-of-plane field B_z at a field strength B_{nuc} and propagated into the notch where it is pinned and stabilized due to $B_{nuc} < B_{dep}$.

Secondly, the out-of-plane field B_z is increased step-wise for different in-plane field pulse amplitudes in order to determine $B_{dep} = B_z + \Delta B_z = f(B_{in-plane})$, the field at which the DW is depinned from the notch. The field-generating current pulses $I_{in-plane}$ are applied as soon as the current out-of-plane field amplitude generated by the external magnet is reached. Thereby, the magnetic moments are tilted according to eq. (5) and as shown in Fig. 1(c), and the DW type may change from Bloch to Néel (Fig. 3) as long as the in-plane field is applied.

C. Results

Figure 5 shows the measured depinning field B_{dep} as function of the applied in-plane field $B_{in-plane}$. The experiment shows an increased drop in B_{dep} after an in-plane field of about 20 mT. For lower values of $B_{in-plane}$ the depinning fields seem to stay more or less constant which is due to the rising out-of-plane field and as suggested from the simulations, due to the change in DW type from a Bloch to Néel wall. For the used range of $B_{in-plane}$ we were able to reduce to B_{dep} by almost 30%, whereas 17% is predicted by the simulations.

The theoretical model for B_{dep} based on eqs. (3), (4) and (5) is in good agreement with experimental and simulation results. Geometry parameters used for calculations and simulations are obtained from the SEM image (Fig. 4).

In the theoretical model only the Bloch DW energy density is used explaining the good agreement with the experiment for low in-plane fields since here the DW is mainly characterized by a Bloch wall. For higher in-plane fields a combination of Bloch and Néel and eventually only a Néel wall is present. Furthermore it is also difficult to predict or determine when the change of DW type actually has taken place. However, simulations indicate the transition at least for high in-plane fields.

For the simulation, the drop in depinning field is less strong than in the experiments and the theoretical model. Possible explanations are that the simulations are carried out without thermal energy or thermal fluctuations, assuming 0 K. Therefore no extra thermal energy, additional to the applied Zeeman energy, is available for the DW to overcome the energy barrier of the notch. Secondly, as observed from the SEM image in Figure 4, the apex angle of the notch is slightly rounded which can cause a difference in the exact pinning spot of the DW between simulation and

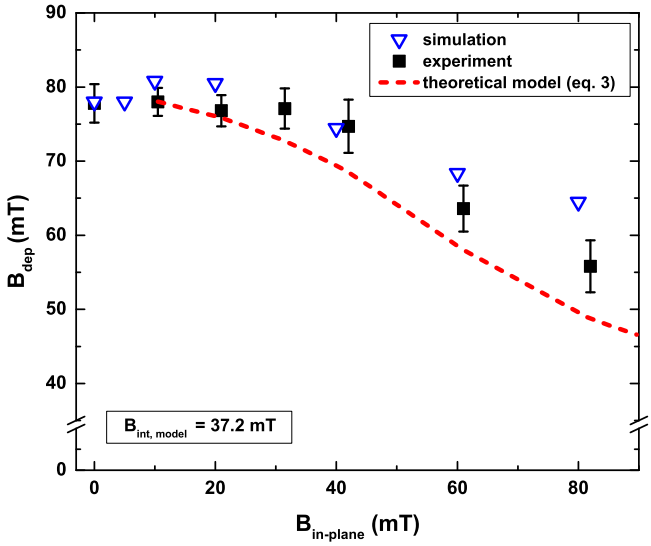

FIG. 5. Measured and calculated out-of-plane depinning field B_{dep} as function of the applied in-plane field $B_{in-plane}$. A decrease is expected and observed since the DW angle is reduced for larger in-plane fields and therefore also the DW energy density and thus depinning field decreases. The theoretical model is in good agreement with both the experiment and micromagnetic simulations. Error bars represent the standard deviation of the measured depinning fields ($N = 10$).

experiment. We achieved a best fit for the model to the experiment by using $\alpha = 24°$, $h = 29\,\text{nm}$, $K_{eff} = 1.47 \cdot 10^5 \text{J/m}^3$ and $A_{ex} = 1 \cdot 10^{-11}\,\text{J/m}$, which is still close to the measured values. Note, the anisotropy of the patterend nanomagnets may vary from the one of the investigated reference multilayer film ($K_{eff} = 1.47 \cdot 10^5 \text{J/m}^3$) due to elevated process temperatures during fabrication or a slight irradiation of the structures during the FIB lithography.

V. CONCLUSION

Experiments and micromagnetic simulations show that the DW depinning from notches can be facilitated by using in-plane magnetic fields to lower the energy barrier of the notch. The out-of-plane depinning field for a DW at the notch is lowered by increasing in-plane field. We achieved a reduction of about 30% in the depinning field during experiments, whereas 17% is predicted by the simulations. These simulations have shown a small increase in B_{dep} at low in-plane field values due to a DW change from Bloch to Néel walls, the latter having a larger energy density.

In summary, we have shown that short in-plane field pulses can be used to decrease the energy barrier of the notch and therefore the depinning field for the DW. Thereby, the in-plane magnetic field pulses in the sub-μs range generated by current pulses through buried current wires are highly suitable to control the signal flow in fast operating pNML systems.

ACKNOWLEDGMENTS

The authors like to thank S. Boche for her valuable input and dedicated help in the cleanroom.

[1] S.S.P. Parkin *et al.*, Science **320**, 190-194 (2008).
[2] R.L. Stamps *et al.*, Journal of Physics D: Applied Physics **47**, 333001 (2014).
[3] D. A. Allwood *et al.*, Science **309**, 1688 (2005).
[4] S. Breitkreutz *et al.*, Journal of Applied Physics **115**, 17D506 (2014).
[5] H.Y. Yuan and X.R. Wang, Physical Review B **89**, 054423 (2014).
[6] S. Breitkreutz *et al.*, EPJ Web of Conferences **75**, 05001 (2014).
[7] S. Breitkreutz *et al.*, IEEE International Electron Devices Meeting (IEDM) (2013), pp. 593-596.
[8] K.-J. Kim and S.-B. Choe, Journal of Magnetism and Magnetic Materials **321**, 2197-2199 (2009).

[9] S. Breitkreutz-v. Gamm, "Perpendicular Nanomagnetic Logic: Digital Logic Circuits from Field-coupled Magnets," Ph.D. thesis, Technische Universität München (2015). Available online: http://nbn-resolving.de/urn/resolver.pl?urn:nbn:de:bvb:91-diss-20150507-1237285-1-0.
[10] R. O'Handley, *Modern Magnetic Materials: Principles and Applications*, ISBN-13: 000-0471155667.
[11] J.M.D. Coey, *Magnetism and Magnetic Materials* (Trinity College, Dublin, 2009), ISBN-13 978-0-511-67743-4.
[12] K.-W. Moon, J.-C. Lee, and S.-B. Choe, Review of Scientific Instruments **80**, 113904 (2009).
[13] A. Gerber *et al.*, Journal of Magnetism and Magnetic Materials **9097**, 242-245 (2002).
[14] http://math.nist.gov/oommf.
[15] J.H. Franken, M. Hoeijmakers, R. Lavrijsen, and H.J.M. Swagten, Journal of Physics: Condensed Matter **24**, 024216 (2012).
[16] R. Lavrijsen, J.H. Franken, J.T. Kohlhepp, H.J.M. Swagten, and B. Koopmans, Applied Physics Letters **96**, 222502 (2010).
[17] Finite Element Method Magnetics Software. Available online: http://www.femm.info.